Received: 2 July 2019 | Revised: 26 August 2019 | Accepted: 18 September 2019

DOI: 10.1002/bio.3718

RESEARCH ARTICLE

LUMINESCENCE The Journal of Biological and Chemical Luminescence WILEY

# A Phenazine based colorimetric and fluorescent chemosensor for sequential detection of $Ag^+$ and $I^-$ in aqueous media

Pravin R. Dongare[1] | Anil H. Gore[2,3] | Govind B. Kolekar[2] | Balu D. Ajalkar[1]

[1]Department of Chemistry, Shivraj College of Arts, Commerce and D. S. Kadam Science College, Gadhinglaj, Affiliated to Shivaji University, Kolhapur, Maharashtra, India

[2]Department of Chemistry, Shivaji University, Kolhapur, Maharashtra, India

[3]Department of Chemistry, Uka Tarsadia University, Mahuva Road, Tarsadi, Bardoli, Gujarat, India

**Correspondence**
Balu D. Ajalkar, Department of Chemistry, Shivraj College of Arts, commerce and D. S. Kadam Science College, Gadhinglaj. Maharashtra, 416502, India.
Email: bajalkar@rediffmail.com

## Abstract

A new colorimetric and fluorescent probe **MNTPZ** based on *1H*-imidazo[*4,5-b*]phenazine derivative has been designed and synthesized for successive detection of $Ag^+$ and $I^-$. The probe **MNTPZ** shows selective colorimetric response by a change in color from yellow to orange and "turn-off" fluorometric response upon binding with $Ag^+$ in DMSO: Water (pH = 7, 1:1, *v/v*) over other cations. The binding mode of probe **MNTPZ** to $Ag^+$ was studied by Job's plot, $^1H$ NMR studies, FT-IR spectroscopy and DFT calculations. Moreover, the situ generated probe **MNTPZ**+ $Ag^+$ complex acted as an efficient fluorometric "turn-on" probe for $I^-$ via $Ag^+$ displacement approach. The detection limit of probe **MNTPZ** for $Ag^+$ and the resultant complex probe **MNTPZ**+ $Ag^+$ for $I^-$ were determined to be 1.36 μmol/L and 1.03 μmol/L respectively. Notably, the developed probe was successfully used for quantitative determination of $I^-$ in real samples with satisfactory results.

KEYWORDS

Aqueous media, Chemosensor, DFT study, Phenazine, Silver

## 1 | INTRODUCTION

In recent year's development of selective and sensitive fluorescent and colorimetric chemosensors recognizing analyte gained considerable attention owing to their vital roles in medical, chemical and environmental applications.[1–5] Among the various metals, silver is an important precious transition metal plays a significant role like anti-infective and antimicrobial agent against a large number of bacteria.[6,7] Likewise, silver and its complexes also widely used in the electric industry, photographic imaging industry, pharmacy, catalyst in oxidation reactions and in the production of jewelry and silverware. However, during such activities large amount of silver is released into an environment which is harmful to aquatic organisms and human body.[8–10] The excessive intake of silver in human body through food chain causes long term insoluble precipitates accumulation in the skin and eyes.[11] Furthermore, silver ions bind with an amine, imidazole and carboxyl groups present in various metabolites and inactivate the sulfhydryl enzymes, leads to harmful effects on human health.[12–14] The United state environmental protection agency (US-EPA) also set a secondary maximum contaminant level to $Ag^+$ in drinking water is 0.93 μmol/L.[15] Hence, it is necessary to develop a method for detection of silver.

Meanwhile, recognition of anion by using a suitable receptor is a growing research area in the field of supramolecular chemistry due to their important role in environmental and biological system.[16,17] Among the various anions, iodide ion received much interest because it is one of the vital micronutrients for normal human growth as it has importance in cell growth, thyroid gland function and brain function.[18] Similarly, elemental iodine is commonly used various fields such as synthesis of drugs, dyes and many other applications which leads to the release of excess iodine causes an adverse effect on the environmental system and human health.[19,20] The, excessive intake or deficiency of iodine causes thyroid dysfunction, mental retardation, increases spontaneous abortion, perinatal death and growth of thyroid cancer.[21,22] WHO also make guidelines about the iodine deficiency as it is a major public health problem cause mental retardation in small children. So, it is greatly important to develop a sensitive and selective method for detection of $I^-$ in environmental and biological samples.

  

In order to detect $Ag^+$ and $I^-$, several modern analytical methods developed such as atomic absorption spectroscopy (AAS),[23] inductively coupled plasma mass spectrometry (ICP-MS),[20,24] electrochemical techniques,[25] ion chromatography.[26] However, chemosensors for detection different ions pay special attention of the researchers of chemical, environmental and medicinal sciences owing to their excellent sensitivity, selectivity, easiness for tuning and low cost for the equipment.[27,28]

At present, a single receptor that can recognize independently both metal ion and anion in the presence of other competitive ions give more interest because it has advantages such as multi-ions detection, more effective analysis and development of molecular system which is useful for the construction of molecular keypad or molecular logic gates.[4,29,30] In addition, a number of sensors reported for the recognition of anions and amino acids by cation displacement approach such as $Ni^{2+}/CN^-$,[31] $Fe^{3+}/CN^-$,[32] $Cu^{2+}/S^{2-}$,[33] $Cu^{2+}$/cysteine,[34] $Ag^+$/proline.[35] However, sensors for the recognition of $Ag^+$ and the resultant metal complex for the recognition of $I^-$ via displacement approach are scarce.[36] Therefore, it is necessary to develop highly selective and sensitive chemosensor that can recognize sequentially $Ag^+$ and $I^-$ in aqueous media.

Phenazine and their derivatives are the nitrogen-containing conjugated heteroaromatic system have been widely used as anticancer, antibiotics and antibacterial agents.[37] Also, due to optical properties phenazine derivatives are useful in electroactive materials like organic light emitting diode (OLED), photoactive materials for solar cells, fluorescent marker and stain for subcellular localizations.[38] Furthermore, in recent year's phenazine derivatives which alter their optical properties upon binding with analyte are reported in the literature.[39–41] Hence, in the present study, we report the synthesis and characterization of phenazine derivative, 2-[3-methyl-5-(4-nitrophenyl)thiophen-2-yl]-*1H*-imidazo[*4,5-b*]phenazine (**MNTPZ)** as a colorimetric and fluorescent probe. The sensing property of this probe **MNTPZ** was tested with a series of alkali, alkaline earth and transition metal ions in DMSO: $H_2O$ media. The formation of probe **MNTPZ**+ $Ag^+$ complex is reversible in the presence of iodide ion and it could be used as an efficient probe for $I^-$ ion.

## 2 | EXPERIMENTAL

### 2.1 | Materials and measurements

*o*-phenylenediamine, 3-methyl-2-thiophenecarboxaldehyde, *p*-nitroaniline were purchased from Sigma-Aldrich and used without further purification. Nitrate and sulphate salts of different cations ($Na^+$, $K^+$, $Mg^{2+}$, $Ca^{2+}$ $Ba^{2+}$, $Al^{3+}$, $Sn^{2+}$, $Pb^{2+}$, $Fe^{2+}$, $Fe^{3+}$, $Co^{2+}$, $Ni^{2+}$, $Cu^{2+}$, $Ag^+$, $Zn^{2+}$, $Cd^{2+}$, $Hg^{2+}$); sodium and potassium salts of anions ($CN^-$, $OAc^-$, $F^-$, $Cl^-$, $Br^-$, $I^-$, $CrO_7^{2-}$, $SO_8^{2-}$, $NO^{2-}$, $SCN^-$, $HPO^-$) were purchased from S. D. Fine-Chem. Ltd. (Mumbai, India). All the analytical grade solvents were purchased from available commercial sources and were used without further purification. The nuclear magnetic resonance spectra ($^1$H-NMR and $^{13}$C-NMR) were recorded on a Bruker AC 300 MHz NMR spectrometer using DMSO-$d_6$ as solvent and tetramethylsilane (TMS) as internal standard ($\delta$ in ppm). The C, H, N analyses were performed on a Vetro-ELIII elemental analyzer. UV–Vis absorption spectra were recorded at room temperature using ELICO SL-210 UV–Vis double beam spectrophotometer using a quartz cell with 1.0 cm path length. The fluorescence spectra were recorded using JASCO (FP-8300, Japan) Spectrofluorophotometer with 1.0 cm quartz cell. Infrared (IR) spectral measurements of samples were recorded on a Perkin Elmer Spectrum Two FT-IR spectrophotometer in the range of 4000–600 $cm^{-1}$ and all pH values were measured by using digital pH-meter with a magnetic stirrer (Equip-Tronics EQ-614 A).

### 2.2 | Synthesis of probe MNTPZ

*2, 3-diamino-phenazine* was prepared according to a reported method.[42]

*5-(4-nitrophenyl)-3-methyl-2-thiophenecarbaldehyde* was synthesized by the reported method.[43,44]

2,3-diamino-phenazine (3.0 mmol) and 5-(4-nitrophenyl)-3-methyl-2-thiophenecarbaldehyde (3.6 mmol) with little quantity of acetic acid were mixed in a 40 mL of hot absolute DMF solvent and the resulting solution was refluxed for 9 hours at 80°C. The progress of the reaction was monitored by TLC (*n*-hexane/ethyl acetate, 2:8, *v/v*), After the completion of reaction, the reaction mixture was cooled to room temperature, precipitate obtained was filtered, washed with ethanol and recrystallized in DMF/$H_2O$ to give brown solid (Scheme 1).

Brown solid, Yield: 83%, M. P. >300°C; $^1$H NMR (300 MHz, DMSO-$d_6$) (**Figure S1**), $\delta$ = 2.301 (s, 3H, $-CH_3$), 7.101 (s, 1H, CH), 7.709–7.331 (d, 2H, HAr), 7.839–7.863 (d, 2H, HAr), 8.150 (s, 2H, HAr), 8.216–8.253 (d, 4H, HAr), 13.473 (s, 1H, NH) ppm; $^{13}$C NMR (75 MHz, DMSO-$d_6$), (**Figure S2**): $\delta$ = 21.03, 109.63, 125.61, 126.84, 127.11, 129.89, 130.10, 130.45, 134.58, 136.91, 140.76, 141.24, 143.32, 144.60, 150.30, 152.29 ppm; Anal. Cal. for $C_{24}H_{15}N_5O_2S$: C, 65.89; H, 3.46; N, 16.01. Found: C, 65.47; H, 3.68; N, 16.18.

### 2.3 | Experimental procedure

A stock solution of probe **MNTPZ** was prepared at $1 \times 10^{-4}$ mol/L in DMSO: $H_2O$ (1:1, *v/v*) and stock solution of salt of different cations and anions ($2 \times 10^{-3}$ mol/L) were prepared in double distilled water. For UV–Vis and fluorescence spectral measurements, the probe **MNTPZ** was further diluted to 5 ml with DMSO: $H_2O$ (pH = 7, 1:1, *v/v*) to give final concentration 10 μmol/L and then absorption and fluorescence spectra were recorded by adding 100 μmol/L of each cation to the solution of probe **MNTPZ**. The fluorescence spectral measurements were carried out at $\lambda_{ex}$ = 458 nm and $\lambda_{em}$ = 551 nm with slit width 5 nm.

**SCHEME 1** Synthesis of probe **MNTPZ**

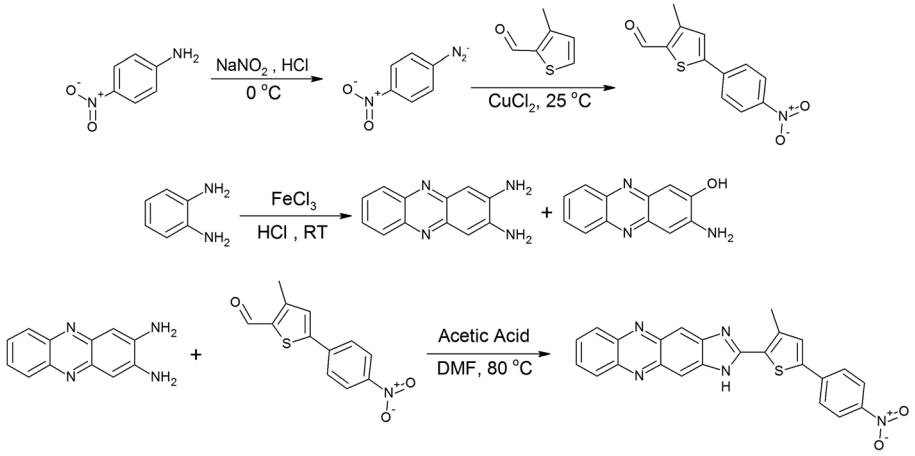


## 3 | RESULT AND DISCUSSION

### 3.1 | UV–vis and fluorescence studies of probe MNTPZ toward metal ions

The colorimetric and fluorescence sensing ability of probe **MNTPZ** was studied in presence of different biologically important metal ions ($Na^+$, $K^+$, $Mg^{2+}$, $Ca^{2+}$ $Ba^{2+}$, $Al^{3+}$, $Sn^{2+}$, $Pb^{2+}$, $Fe^{2+}$, $Fe^{3+}$, $Co^{2+}$, $Ni^{2+}$, $Cu^{2+}$, $Ag^+$, $Zn^{2+}$, $Cd^{2+}$, $Hg^{2+}$) by using UV–Vis absorption and fluorescence spectroscopic techniques in DMSO:$H_2O$ (1:1, *v*/*v*), bis-Tris buffer (pH = 7) medium.

As shown in Figure 1a the UV–Vis absorption spectrum of free probe **MNTPZ** exhibited maximal absorbance at 287 nm and 429 nm. Upon the addition of 100 μmol/L of each metal ions into the solution of probe **MNTPZ** (10 μmol/L), little or no significant changes occur in the absorption peak of probe **MNTPZ** in the presence of different ions. However, in presence of $Ag^+$ ion the absorbance peak of probe **MNTPZ** decreases at 429 nm and a new absorption peak emerge at 513 nm with red shift and showed a naked eye color change from yellow to orange in aqueous solution (Figure 1b).

The studies of interaction between probe **MNTPZ** (10 μmol/L) and various metal ions were further monitored by the fluorescence spectroscopy in DMSO: $H_2O$ (1:1, *v*/*v*) bis-Tris buffer (pH = 7) at an excited wavelength of 458 nm. Figure 2a shows, the free probe exhibits maximum emission at wavelength 551 nm with a fluorescence quantum yield (φ) value 0.64. The addition of 100 μmol/L of various metal ions to the solution of probe **MNTPZ** (10 μmol/L), only $Ag^+$ into a solution of probe **MNTPZ** gives quenching of fluorescence and most of the metal ions showed an either no or bit changes in fluorescence intensity of probe **MNTPZ**. The decrease in intensity of fluorescence is may be attributed to intramolecular charge transfer (ICT) by binding of $Ag^+$ to imidazole and thiophene moiety of probe **MNTPZ**. Importantly this turn-off fluorescence of probe **MNTPZ** by $Ag^+$ can be seen by the naked eye under UV light from greenish yellow to colorless (Figure 2b).

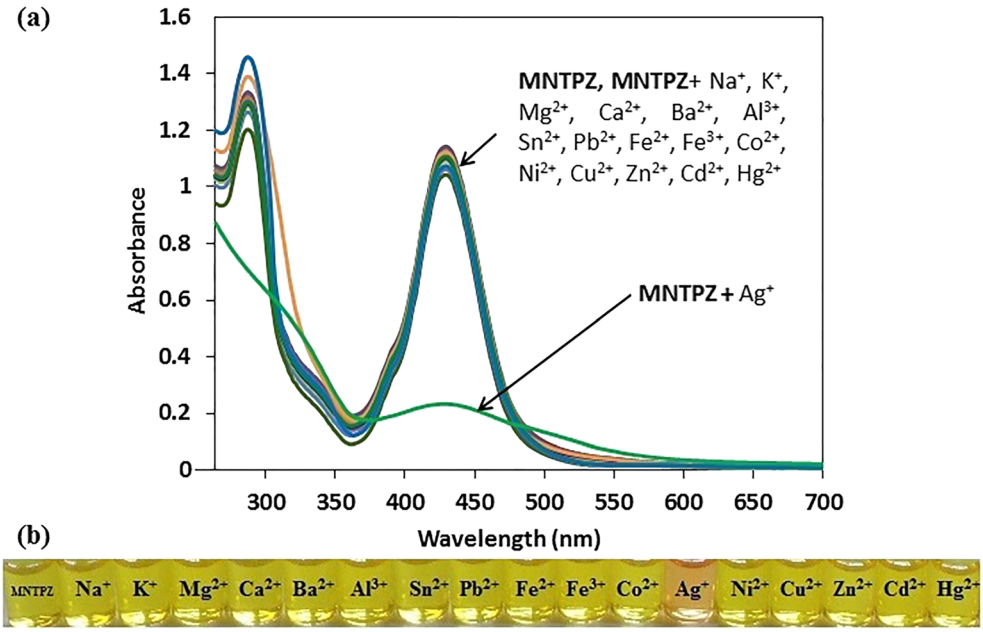


**FIGURE 1** (a) UV–vis spectra of probe **MNTPZ** (10 μmol/L) in the presence of different cations (100 μmol/L) in DMSO:$H_2O$ (1:1, *v*/*v*), bis-Tris buffer (pH = 7) solution and (b) corresponding color changes

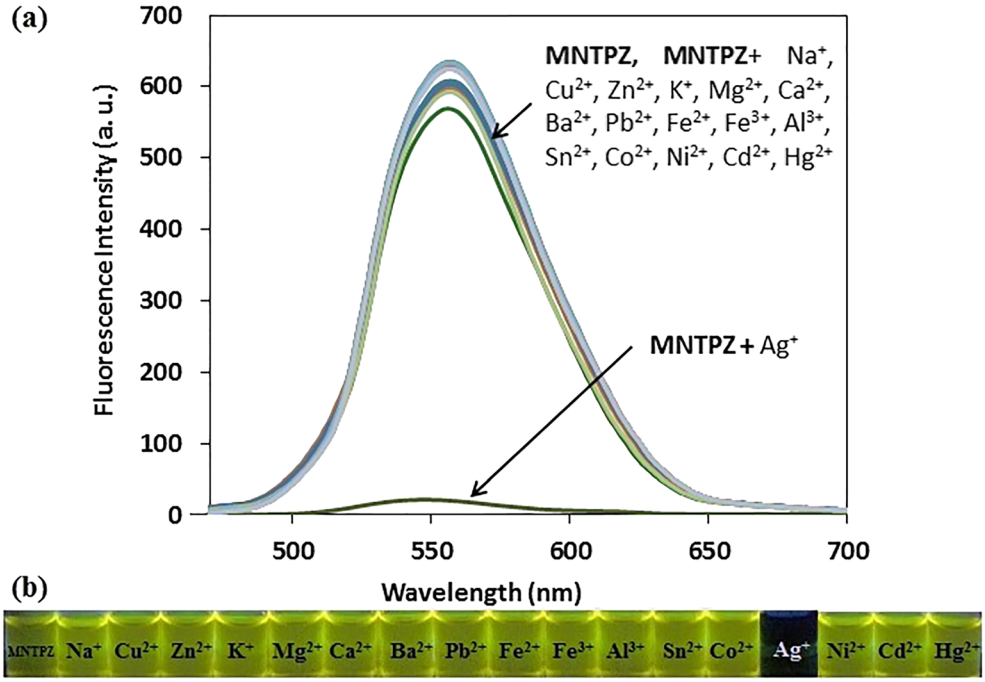


**FIGURE 2** Fluorescence spectra of probe **MNTPZ** (10 μmol/L) in the presence of different metal ions (100 μmol/L) in DMSO:$H_2O$ (1:1, *v*/*v*), bis-Tris buffer (pH = 7) solution and corresponding UV irradiation images

Based on the selectivity of probe **MNTPZ** towards $Ag^+$, the binding behavior was investigated by UV–Vis titration experiment (Figure 3). On the incremental addition of $Ag^+$ to the solution of probe **MNTPZ**, the absorbance band at 287 and 429 nm slowly decreased and a new red shift absorption band emerges at 513 nm with an isosbestic point at 306 and 488 nm. The red shift of the absorption band might be due to internal charge transfer (ICT), which is responsible for dramatic color change from yellow to orange upon binding of probe **MNTPZ** with $Ag^+$.

Furthermore, the interaction between probe **MNTPZ** and $Ag^+$ were studied by fluorescence titration experiment ($\lambda_{ex}$ = 458 nm). Figure 4 shows, with increasing concentration of $Ag^+$ from 0.0 to 100 μmol/L into the solution of probe **MNTPZ** the intensity of fluorescence emission peak at 551 nm gradually decreased and the fluorescence intensity of probe **MNTPZ** was almost quenched (quenching efficiency $(I_0–I)/I_0 \times 100\%$ = 99%) by addition of 60 μmol/L of $Ag^+$. The quenching of fluorescence is due to heavy atom effect and by intramolecular charge transfer (ICT) process.

## 3.2 | Metal ion competition studies

To explore the pivotal requirement of the probe **MNTPZ** for its practical applications competition experiment were carried out in the

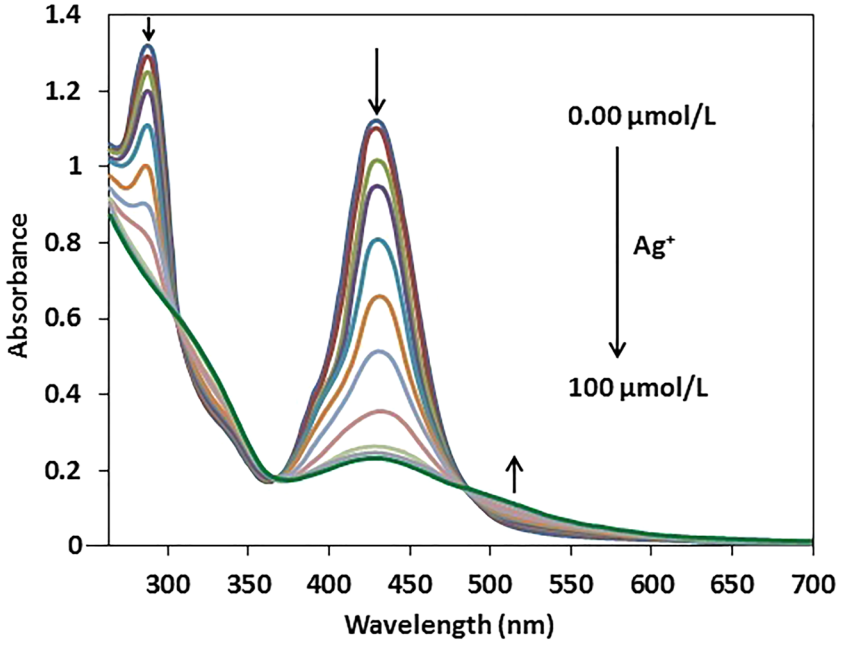


**FIGURE 3** UV–visible spectral changes of probe **MNTPZ** (10 μmol/L) with increasing concentrations of $Ag^+$ in DMSO:$H_2O$ (1:1, *v*/*v*), bis-Tris buffer (pH = 7) solution

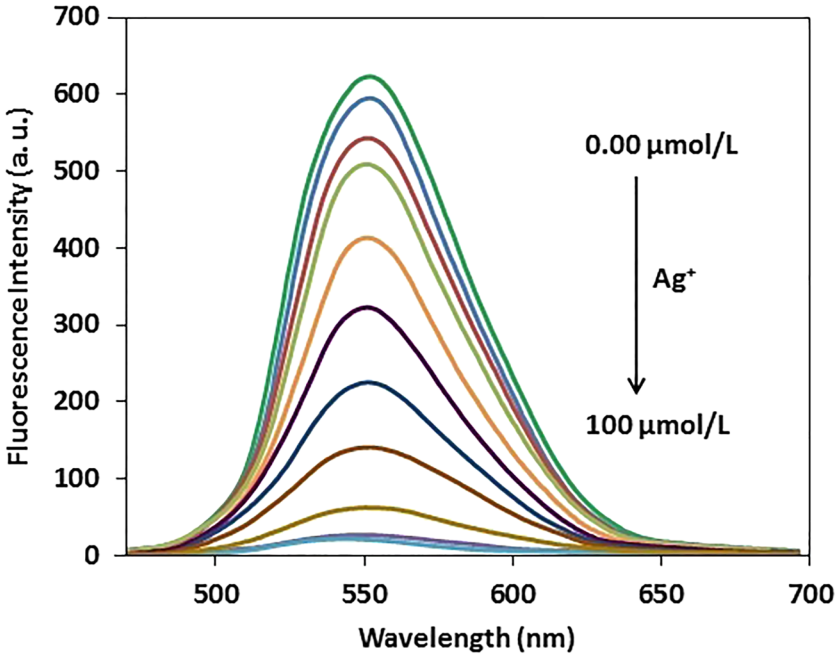


**FIGURE 4** Fluorescence titration spectrum of probe **MNTPZ** (10 µmol/L) upon gradual addition of $Ag^+$ (0.0–100 µmol/L) in DMSO:$H_2O$ (1:1, *v/v*), bis-Tris buffer (pH = 7) solution

presence of coexisting metal ions by UV–Vis and fluorescence method. For this purpose, solution of probe **MNTPZ** in DMSO: $H_2O$ (1:1, *v/v*), bis-Tris buffer (pH = 7) was prepared and aliquots of $Ag^+$ (100 µmol/L) and other metal ions (100 µmol/L) were added. The bar diagram (Figure 5 and Figure 6) shows UV–Vis absorption and fluorescence ($\lambda_{ex}$ = 458 nm) response of probe **MNTPZ**+ $Ag^+$ in absence and presence of coexisting cations. It is seen that, little or negligible changes occur in absorption and fluorescence spectrum of probe in

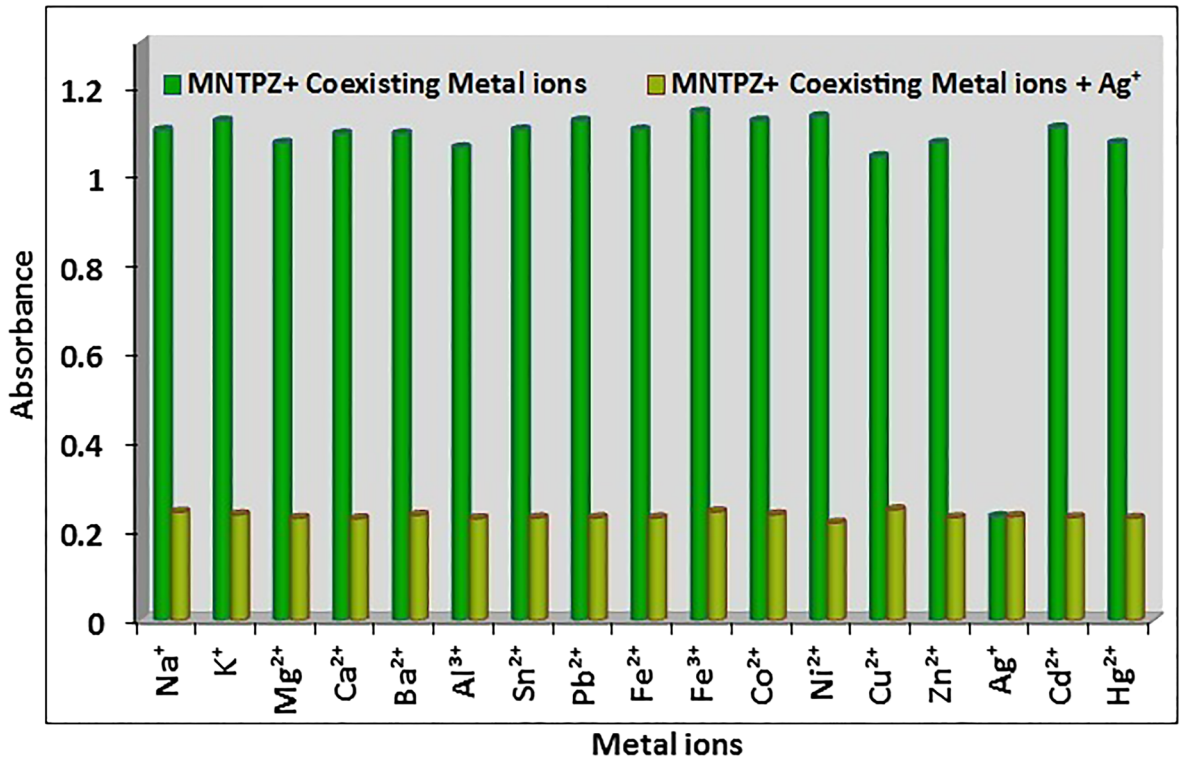


**FIGURE 5** Absorbance responses of probe **MNTPZ** in the absence and presence of $Ag^+$ ions (100 µmol/L) and several competing cations like $Na^+$, $K^+$, $Mg^{2+}$, $Ca^{2+}$, $Ba^{2+}$, $Al^{3+}$, $Sn^{2+}$, $Pb^{2+}$, $Fe^{2+}$, $Fe^{3+}$, $Co^{2+}$, $Ni^{2+}$, $Cu^{2+}$, $Zn^{2+}$, $Ag^+$, $Cd^{2+}$, $Hg^{2+}$ (100 µmol/L) in DMSO:$H_2O$ (1:1, *v/v*), bis-Tris buffer (pH = 7) solution at wavelength 429 nm. The green bars represent the absorbance response of probe **MNTPZ** in the presence of competing metal ions (100 µmol/L). The yellow bars represent the absorbance response of probe **MNTPZ**

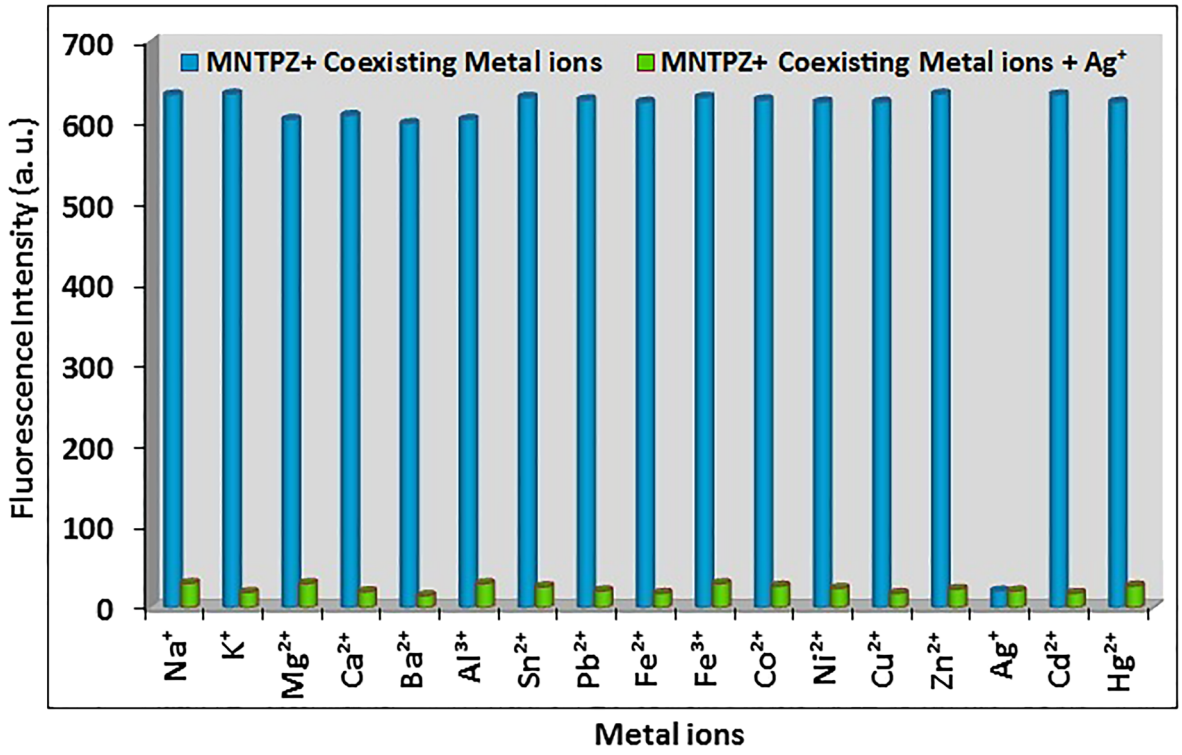


**FIGURE 6** Fluorescence responses of probe **MNTPZ** in the absence and presence of $Ag^+$ ions (100 μmol/L) and several competing cations like $Na^+$, $K^+$, $Mg^{2+}$, $Ca^{2+}$, $Ba^{2+}$, $Al^{3+}$, $Sn^{2+}$, $Pb^{2+}$, $Fe^{2+}$, $Fe^{3+}$, $Co^{2+}$, $Ni^{2+}$, $Cu^{2+}$, $Zn^{2+}$, $Ag^+$, $Cd^{2+}$, $Hg^{2+}$ (100 μmol/L) in DMSO:$H_2O$ (1:1, *v/v*), bis-Tris buffer (pH = 7) solution at $\lambda_{em}$ = 551 nm. The blue bars represent the fluorescence response of probe **MNTPZ** in the presence of competing metal ions (100 μmol/L). The green bars represent the fluorescence response of probe **MNTPZ**

the presence of coexisting metal ions. So, it shows excellent selectivity for $Ag^+$ over other cations.

### 3.3 | Calibration curve, detection limit, stoichiometry of silver ion complexation and binding constant

Quantitative analysis was achieved by titrating a standard solution of $Ag^+$ ions and monitoring the UV–Vis absorption and fluorescence spectra. Initially, UV–Visible absorbance experimental data recorded at wavelength 429 nm for $Ag^+$, were plotted to obtain a linear relationship. Here, a linear correlation occurred in the calibration graph ($A_0$-A) and the concentration of $Ag^+$ ions in the range 0.0 to 30 μmol/L with correlation coefficient 0.9961 (Figure 7). After the addition of more than 30 μmol/L of $Ag^+$, curve reaches a platform and no variation is occurred in the intensity of absorption spectra (**Figure S3**). Importantly, the plot of ($A_0$-A) against the concentration of $Ag^+$ fit a linear Beer–Lambert equation.

Similarly, from fluorescence titration data a linear calibration curve ($F_0$-F) is plotted as a function of change in the concentration of $Ag^+$ (Figure 8). This method gives a better linear relationship between range 0.0 to 30 μmol/L with correlation coefficient 0.9952.

The colorimetric and fluorescence detection limit of this method is 1.99 μmol/L and 1.36 μmol/L calculated by equation (1),[45]

$LOD = \frac{3}{k}$ (1) Where, σ is the standard deviation of the y-intercept of the regression line and k is the slope of a calibration curve.

The stoichiometry of probe **MNTPZ** and $Ag^+$ ion complex was evaluated by Job's plot by keeping the sum of the concentration of $Ag^+$ and probe **MNTPZ** constant and varying the mole fraction from 0.1 to 0.9. The Job's plot[4] gives maximum mole fraction at 0.33

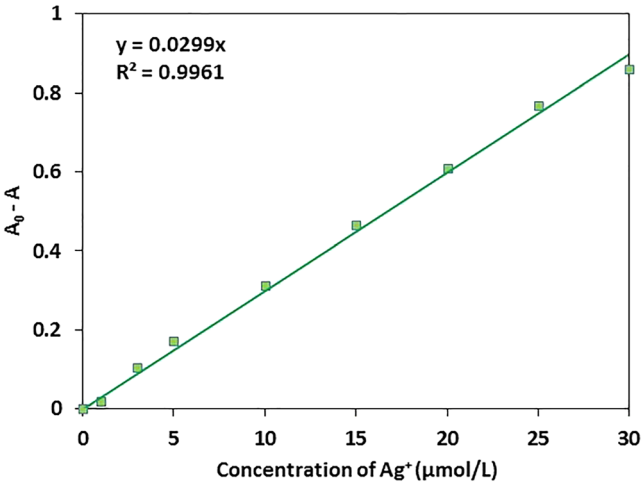


**FIGURE 7** Calibration plot of the $A_0$–A versus concentration of $Ag^+$ shows that system is linear in between 0.0 to 30 μmol/L with probe **MNTPZ** (10 μmol/L) at 429 nm

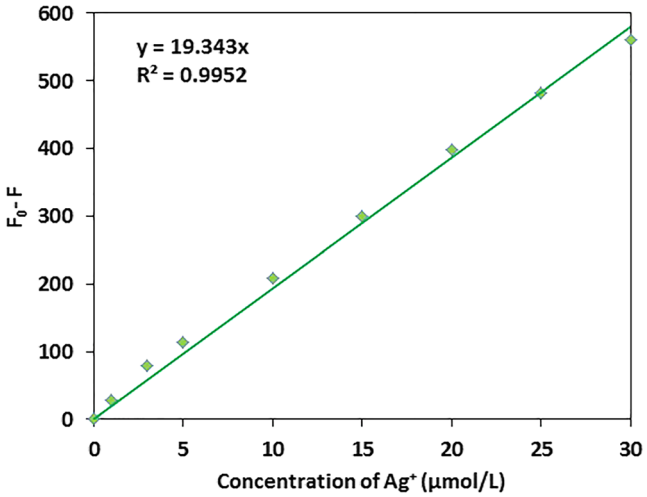


**FIGURE 8** Calibration plot of the $F_0$–F versus concentration of $Ag^+$ shows that system is linear in between 0.0 to 30 µmol/L with probe **MNTPZ** (10 µmol/L) at $\lambda_{ex}$ = 458 nm, $\lambda_{em}$ = 551 nm

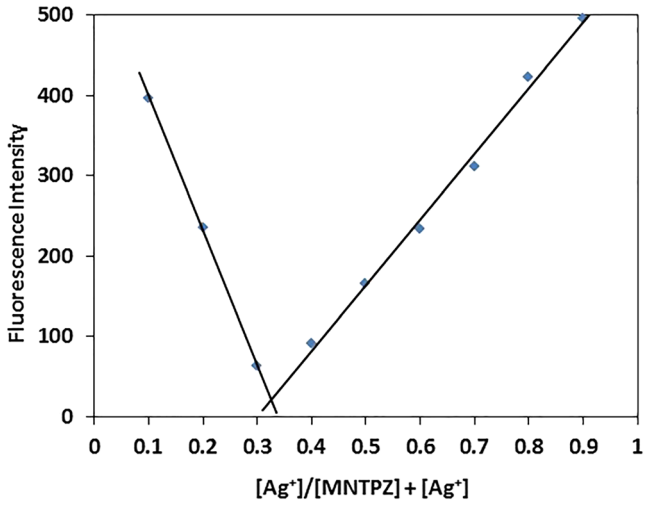


**FIGURE 9** Job's plot showing 2:1 complex formed between probe **MNTPZ** and $Ag^+$ in DMSO:$H_2O$ (1:1, *v*/*v*), bis-Tris buffer (pH = 7) solution at ($\lambda_{ex}$ = 458 nm, $\lambda_{em}$ = 551 nm)

signifying 2:1 stoichiometry between probe **MNTPZ** and $Ag^+$ complex (Figure 9).

Furthermore, the metal binding constant was determined by fluorescence titration response using Benesi-Hildebrand equation (2),[46]

$$\frac{1}{F_0 - F} = \frac{1}{Ka(F_0 - F_{min})[Ag^+]} + \frac{1}{F_0 - F_{min}} \quad (2)$$

From the slope and intercept of line binding constant is found to be Ka = 2.25 × $10^4$ $M^{-1}$ shows effective binding between probe **MNTPZ** and $Ag^+$ (**Figure S4**).

## 3.4 | Fluorescence studies of probe MNTPZ+ $Ag^+$ towards anions

In order to further recognize the sensing ability of probe **MNTPZ**+ $Ag^+$ towards anions, the in situ generated probe **MNTPZ**+ $Ag^+$ complex was directly employed to detect anion by using fluorescence method in DMSO: $H_2O$ (1:1, *v*/*v*, pH = 7) solution. Figure 10a shows fluorescence spectra of probe **MNTPZ**+ $Ag^+$ emitted weakly at 551 nm, by the addition of 100 µmol/L of $I^-$ to probe **MNTPZ**+ $Ag^+$ complex, the fluorescence intensity was enhanced rapidly nearly to the level of free probe **MNTPZ** and the fluorescence color changes from colorless to greenish yellow seen by the naked eye under a UV lamp (Figure 10b). However, other anions including $OAc^-$, $F^-$, $Cl^-$, $Br^-$, $Cr_2O_7^{2-}$, $S_2O_8^{2-}$, $NO_3^{2-}$, $SCN^-$, $H_2PO_4^-$ not produce any significant changes in fluorescent intensity.

Furthermore, to evaluate the interaction of probe **MNTPZ**+ $Ag^+$ with $I^-$ fluorescence titration study was executed by keeping the concentration of $Ag^+$ (100 µmol/L) constant in probe **MNTPZ** with increasing concentration of $I^-$. As shown in Figure 11, the fluorescence intensity of probe **MNTPZ**+ $Ag^+$ complex increases linearly at 551 nm from concentration 0.0 to 100 µmol/L of $I^-$ indicating that probe **MNTPZ**+ $Ag^+$ complex has highly sensitive and selective detection ability for $I^-$.

Moreover, in order to explore the practical application of probe **MNTPZ**+ $Ag^+$ complex as a selective probe for $I^-$ competitive experiment was carried out in the presence of competitive anions. As shown in Figure 12 the fluorescence intensity enhancement is shown only in the presence of $I^-$. While no other anions show substantial changes in fluorescence intensity.

## 3.5 | Calibration curve, detection limit and binding constant for $I^-$

A linear calibration curve ($F-F_0$) is plotted as a function of change in concentration of $I^-$ shown in **Figure S5**. The plot shows that the change in fluorescence intensity is increased in a linear function with the concentration of $I^-$ in the range 0.0 to 15 µmol/L with correlation coefficient 0.9947. The fluorescence limit of detection calculated by equation (1) found to be 1.03 µmol/L.

The stoichiometry of newly formed complex probe **MNTPZ**+ $Ag^+$ and $I^-$ ion was further studied by keeping the sum of the concentration of $I^-$ and probe **MNTPZ**+ $Ag^+$ constant and varying the mole fraction from 0.1 to 0.9. The Job's plot (**Figure S6**) gives maximum mole fraction at 0.5 signifying 1:1 stoichiometry between probe **MNTPZ**+ $Ag^+$ and $I^-$ complex.

Furthermore, the metal binding constant was determined by fluorescence titration response using Benesi-Hildebrand equation (3),[46]

$$\frac{1}{F - F_0} = \frac{1}{Ka(F_{min} - F_0)[I^-]} + \frac{1}{F_{min} - F_0} \quad (3)$$

From the slope and intercept of line binding constant is found to be Ka = 4.66 × $10^4$ $M^{-1}$ (**Figure S7**).

Importantly, **Table S1** has been created to show a comparison data of proposed probe with previously reported sensor for detection of $Ag^+$ and $I^-$.

## 3.6 | Effect of pH

In order to investigate practical application of a successful chemosensor for detection of metal ions at suitable pH condition, we studied

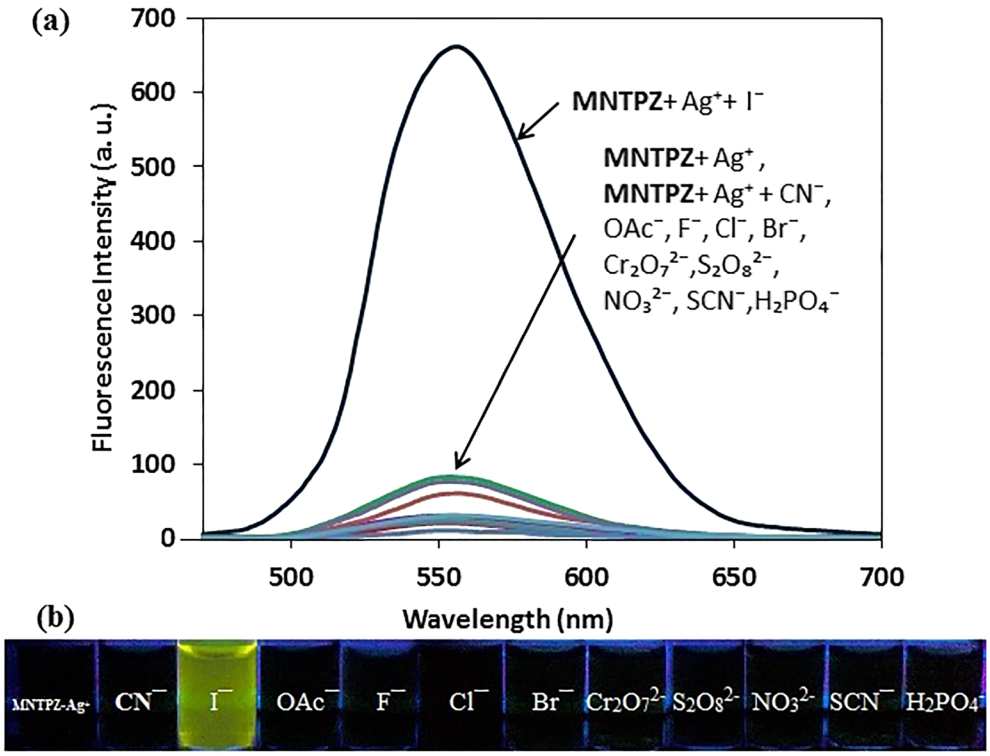


**FIGURE 10** (a) Fluorescence spectra of probe **MNTPZ**+ $Ag^+$ (10 μmol/L) in the presence of different anions (100 μmol/L) in DMSO:$H_2O$ (1:1, *v*/*v*), bis-Tris buffer (pH = 7) solution and (b) corresponding color changes

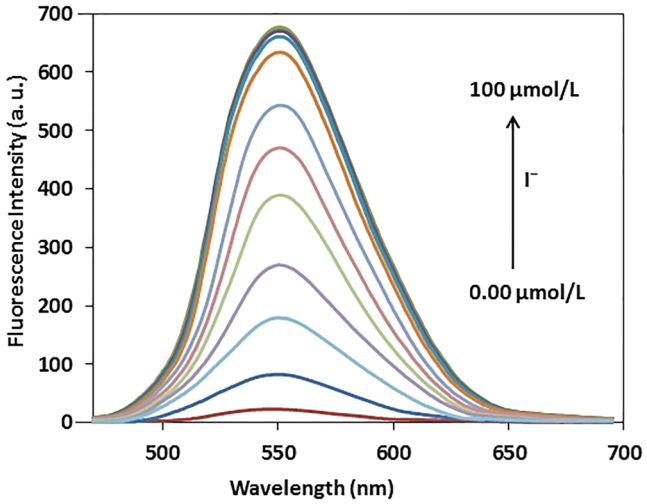


**FIGURE 11** Fluorescence titration spectrum of probe **MNTPZ**+ $Ag^+$ complex (10 μmol/L) upon the gradual addition of $I^-$ (0.0–100 μmol/L) in DMSO:$H_2O$ (1:1, *v*/*v*), bis-Tris buffer (pH = 7) solution

the effect of pH on the fluorescence and absorbance response of probe **MNTPZ**, probe **MNTPZ**+ $Ag^+$ and probe **MNTPZ**+ $Ag^+$ complex to $I^-$ in DMSO: $H_2O$ (1:1, *v*/*v*) in the pH values ranging from 2 to 12 by using bis-Tris buffer. As shown in **Figure S8**, probe **MNTPZ** exhibit strong fluorescence in pH range 3–9 at wavelength 551 nm. However, in presence $Ag^+$ ions the fluorescence intensity of probe **MNTPZ** quenched, when fluorescence intensity of probe **MNTPZ** was quenched. The quenching of fluorescence intensity occurred in the acidic and in basic pH value is due to the proton induced quenching at benzimidazole moiety and hydrolysis of metal ions under the basic conditions respectively. Similarly, probe **MNTPZ**+ $Ag^+$ complex with $I^-$ shows fluorescence enhancement in pH range 3–10. Moreover, from **Figure S9**, probe **MNTPZ** and its $Ag^+$ complex shows a quite stable wide range of pH from 3 to 10 for UV–Visible absorbance taken at wavelength 429 nm response indicates that, probe **MNTPZ** binds with $Ag^+$ over a wide range of pH. Thus, in the present work we choose pH = 7.0 as the most favorable pH for the probe **MNTPZ** in all over the experiment.

## 3.7 | $^1$H NMR titration experiments and IR studies

To study the nature of interaction between the probe **MNTPZ** and silver ion, $^1$H NMR titration experiments and FT-IR study were conducted. **Figure S10** shows the $^1$H NMR spectra of probe **MNTPZ** in the absence and presence of $Ag^+$ in DMSO-$d_6$. When 20 μmol/L of $Ag^+$ was added to probe **MNTPZ**, the proton signal of imidazole –NH group at $\delta$ = 13.473 (s, 1H, NH) ppm completely disappeared and the protons of phenazine and thiophene ring involved in delocalization shows small up field shifts. This shows that an intramolecular charge transfer (ICT) from phenazine ring to thiophene moiety by the interaction of $Ag^+$. Furthermore, the IR spectra of probe **MNTPZ** and its coordinated complex were recorded in order to understand the sensing mechanism of probe **MNTPZ** to $Ag^+$. As shown in **Figure S11**, the IR spectrum of probe **MNTPZ** exhibited three stretching vibration absorption peaks of imidazole N-H, imidazole C=N and thiophene C=C groups that appeared at 3255, 1673 and 1620 $cm^{-1}$ respectively. However, upon coordination of probe **MNTPZ** with $Ag^+$ ion the stretching vibration peak of imidazole N-H disappeared. Meanwhile,

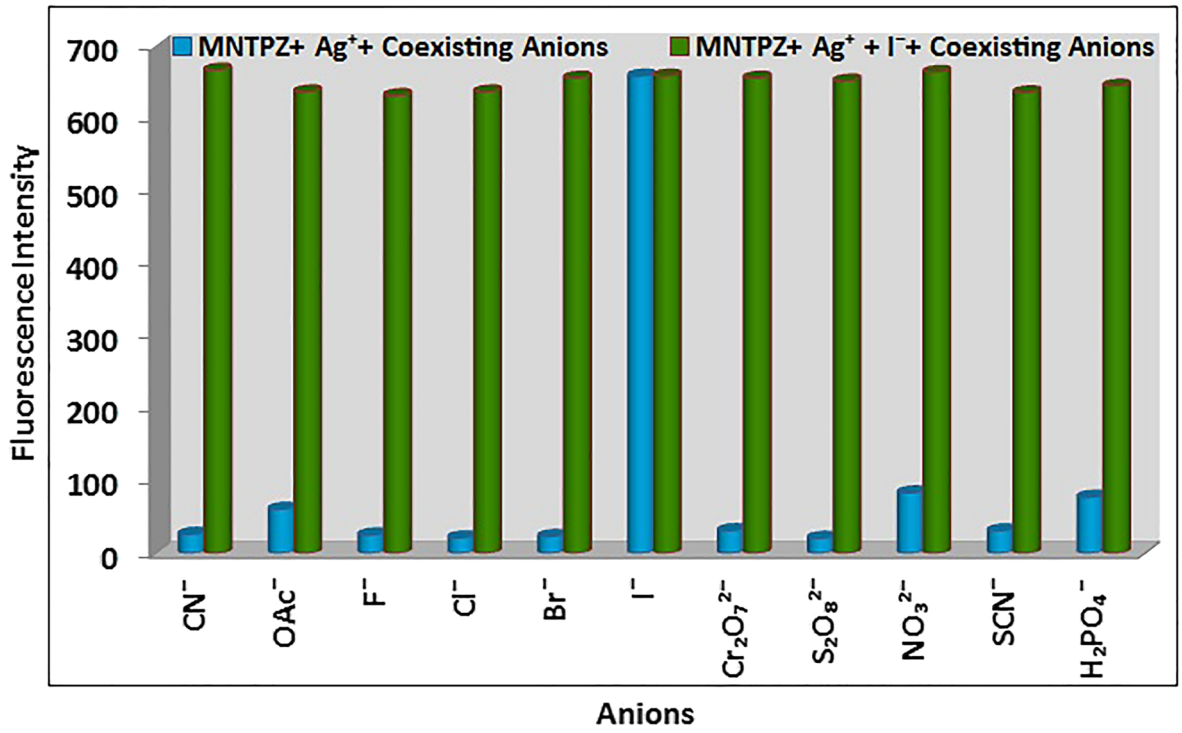


**FIGURE 12** Fluorescence responses of probe **MNTPZ**+ $Ag^+$ in absence and presence of $I^-$ ions (100 μmol/L) and several competing cations like $OAc^-$, $F^-$, $Cl^-$, $Br^-$, $Cr_2O_7^{2-}$, $S_2O_8^{2-}$, $NO_3^{2-}$, $SCN^-$, $H_2PO_4^-$ (100 μmol/L) in DMSO:$H_2O$ (1:1, *v*/*v*), bis-Tris buffer (pH = 7) solution at $\lambda_{em}$ = 551 nm. The blue bars represent the fluorescence response of probe **MNTPZ**+ $Ag^+$ in presence of competing metal ions (100 μmol/L) and green bars represent the fluorescence response of probe **MNTPZ**+ $Ag^+$ upon the addition of competing metal ions and $I^-$

the stretching vibration peaks of imidazole C=N and thiophene C=C shifted to higher wavenumber 1711 and 1638 $cm^{-1}$ respectively, indicated $Ag^+$ had complexation with imidazole N-H nitrogen and sulfur atom of thiophene.

## 3.8 | DFT studies

In order to understand the coordination of probe **MNTPZ** with $Ag^+$ density functional calculations (DFT) calculation performed by using ORCA program package (version 3.0.3, developed by Prof. Dr. Frank Neese).[47] The geometries of probe **MNTPZ** and probe **MNTPZ**+ $Ag^+$ were optimized by using Beck-3 Lee Young Parr (B3LYP)/def2-TZVP and B3LYP/def2-SVP with effective core potential (ECP) based basis set respectively.[48–52] The geometry optimized structure of probe **MNTPZ** and probe **MNTPZ**+ $Ag^+$ along with bond lengths Ag-N (2.13 Å) and Ag-S (2.45 Å) are shown in Figure 13 and Figure 14, the probe **MNTPZ**, HOMO–LUMO analysis revealed that the electron density of HOMO is mainly present on the *1H*-Imidazo[*4,5-b*]Phenazine ring part and LUMO is entirely spread over the whole molecule. While in probe **MNTPZ**+ $Ag^+$ complex HOMO is present over the both *1H*-Imidazo[*4,5-b*]Phenazine rings and electron density in LUMO is localized on the molecule as well as $Ag^+$ ion predicting the ICT and slight LMCT transitions. Furthermore, the energy band gap (ΔE) between HOMO and LUMO of probe **MNTPZ** and corresponding

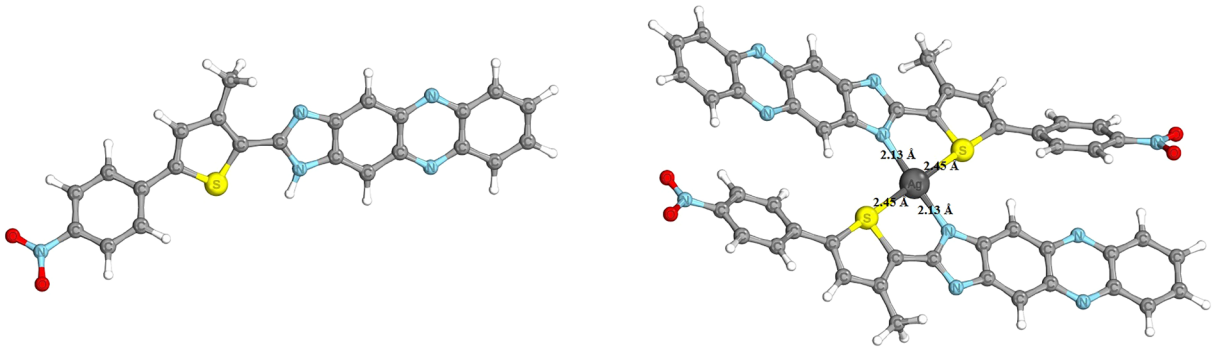


**FIGURE 13** Geometry optimized structure of (a) probe **MNTPZ** and (b) probe **MNTPZ**+ $Ag^+$ complex

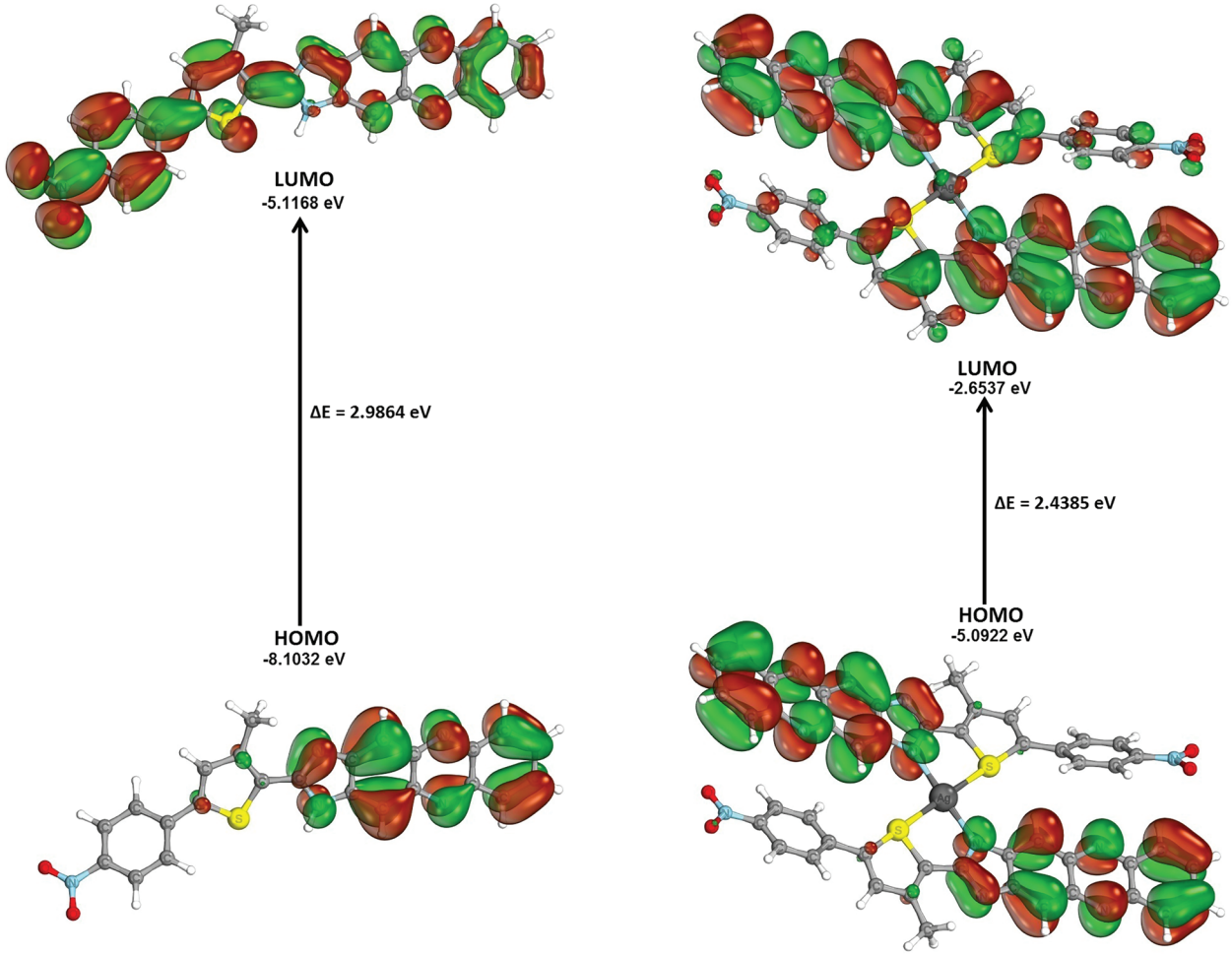


**FIGURE 14** HOMO and LUMO energy level of (a) probe **MNTPZ** and (b) probe **MNTPZ**+ $Ag^+$

probe **MNTPZ**+ $Ag^+$ complex were found to be 2.9864 eV and 2.4385 eV respectively. The lowering of HOMO–LUMO energy gap upon binding with $Ag^+$ is due to the intramolecular charge transfer (ICT) between the probe **MNTPZ** and $Ag^+$ ions which is in closed agreement with the new charge transfer absorption band observed at 457 nm in the UV–Visible spectra.

Thus by considering the above results, the plausible sensing mechanism of probe **MNTPZ** for $Ag^+$ and $I^-$ was shown in Scheme 2.

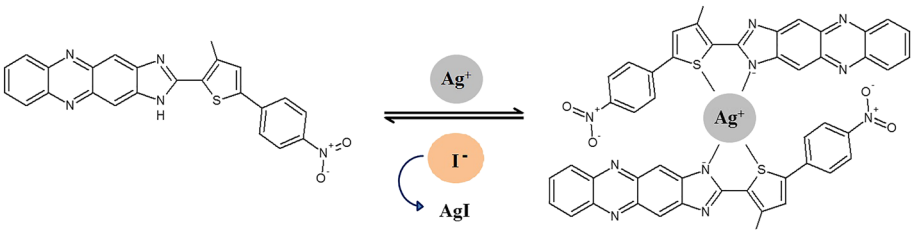


**SCHEME 2** Proposed binding mode of probe **MNTPZ** for $Ag^+$ and $I^-$

**TABLE 1** Determination of $I^-$ in different samples via a standard addition method ($n$ = 3)

| Name of the sample | Amount of standard $I^-$ added (μmol/L) | Total $I^-$ found (n = 3) (μmol/L) | Recovery of $I^-$ added (n = 3) (%) | RSD (%) |
|---|---|---|---|---|
| *tap water | 10.0 | 10.65 | 106.53 | 4.90 |
| | 30.0 | 30.69 | 102.33 | 0.54 |
| **urine sample | 10.0 | 11.13 | 111.23 | 0.83 |
| | 30.0 | 31.56 | 105.21 | 1.67 |

*Hiranyakeshi River, Gadhinglaj, Kolhapur, Maharashtra, India.
**Sub District Hospital, Gadhinglaj.

### 3.9 | Analytical applications of the proposed probe MNTPZ in real a sample for $I^-$

To demonstrate the practical applications of the proposed method, experiments were performed to determine the concentration of $I^-$ in real sample by using standard addition method; water sample is collected from a local region of campus filtered through a Whatman No. 41 filter paper to remove suspended impurities. Similarly, urine samples are obtained from the local hospital of verified healthy unknown volunteers and patient. These three samples were spiked with standard $I^-$ at different concentration levels and further diluted with distilled water to obtain the proper concentration of sample solutions within working linear range and analyzed with the proposed method. The results are listed in Table 1 which is in good agreement with the average recovery of the spiked sample which showed that, probe **MNTPZ** used for determination of $I^-$ in a real sample.

## 4 | CONCLUSIONS

In conclusion, a simple and sensitive phenazine based fluorescent and colorimetric probe **MNTPZ** has been developed for recognition of $Ag^+$ with a low detection limit in mixed aqueous solution. Probe **MNTPZ** showed selectivity toward $Ag^+$ in a 2:1 stoichiometric manner, which induces a visible color change from yellow to orange with a notable bathochromic shift elucidated by the change of ICT band. Furthermore, the chemosensing ensemble probe **MNTPZ**+ $Ag^+$ was used as a fluorescent probe for $I^-$ detection by means of metal displacement approach with a detection limit 1.03 μmol/L in presence of coexisting anions. Moreover, probe **MNTPZ**+ $Ag^+$ ensemble exhibit good water solubility, biocompatibility and stability under a wide pH physiological conditions thus the proposed probe **MNTPZ** was successfully used for the determination of $I^-$ ion with satisfactory results.

### ACKNOWLEDGEMENTS

Authors are thankful to Shivraj College, Gadhinglaj; Department of Chemistry, Shivaji University, Kolhapur and SAIF CSIR-CDRI, Lucknow, India for providing all necessary infrastructural and instrumental facility.

### ORCID

*Balu D. Ajalkar* https://orcid.org/0000-0003-0908-4493

### REFERENCES

[1] K. P. Carter, A. M. Young, A. E. Palmer, *Chem. Rev.* **2014**, *114*, 4564.
[2] M. Wenzel, J. R. Hiscock, P. A. Gale, *Chem. Soc. Rev.* **2012**, *41*, 480.
[3] J. Du, M. Hu, J. Fan, X. Peng, *Chem. Soc. Rev.* **2012**, *41*, 4511.
[4] G. J. Park, I. H. Hwang, E. J. Song, H. Kim, C. Kim, *Tetrahedron* **2014**, *70*, 2822.
[5] J. F. Zhang, Y. Zhou, J. Yoon, J. S. Kim, *Chem. Soc. Rev.* **2011**, *40*, 3416.
[6] A. P. Richter, J. S. Brown, B. Bharti, A. Wang, S. Gangwal, K. Houck, E. A. Cohen Hubal, V. N. Paunov, S. D. Stoyanov, O. D. Velev, *Nat. Nanotechnol.* **2015**, *10*, 817.
[7] S. Eckhardt, P. S. Brunetto, J. Gagnon, M. Priebe, B. Giese, K. M. Fromm, *Chem. Rev.* **2013**, *113*, 4708.
[8] R. Foldbjerg, P. Olesen, M. Hougaard, D. A. Dang, H. J. Hoffmann, H. Autrup, *Toxicol. Lett.* **2009**, *190*, 156.
[9] J. L. Barriada, A. D. Tappin, E. H. Evans, E. P. Achterberg, *TrAC, Trends Anal. Chem.* **2007**, *26*, 809.
[10] Probe Design and Chemical Sensing, in *Topics in Fluorescence Spectroscopy*, (Ed: J. R. Lakowicz) Vol. 4, Plenum Press, New York **1994**.
[11] E. Merian (Ed), *Metals and their Compounds in the environment: occurrence, analysis and biological relevance*, VCH Verlagsgesellschaft mbH, Germany **1991**.
[12] H. Peng, B. W. Brooks, R. Chan, O. Chyan, T. W. La Point, *Chemosphere* **2002**, *46*, 1141.
[13] S. Y. Liau, D. C. Read, W. J. Pugh, J. R. Furr, A. D. Russell, *Lett. Appl. Microbiol.* **1997**, *25*, 279.
[14] Q. L. Feng, J. Wu, G. Q. Chen, F. Z. Cui, T. N. Kim, J. O. Kim, J. Biomed, *Mater. Res.* **2000**, *52*, 662.
[15] National Primary Drinking Water Regulations: Final Rule, U.S.: Environment Protection Agency, **1991** Fed Reg 56:3526.
[16] R. Martinez-Manez, F. Sancenon, *Chem. Rev.* **2003**, *103*, 4419.
[17] R. M. Duke, E. B. Veale, F. M. Pfeffer, P. E. Kruger, T. Gunnlaugsson, *Chem. Soc. Rev.* **2010**, *39*, 3936.
[18] G. Dai, O. Levy, N. Carrasco, *Nature* **1996**, *379*, 458.
[19] B. S. Hetzel, *Bull World Health Organ* **2002**, *80*, 410.
[20] B. Basumatary, M. A. Kaloo, V. K. Singh, R. Mishra, M. Murugavel, J. Sankar, *RSC Adv.* **2014**, *4*, 28417.
[21] L. Patrick, *Altern Med Rev.* **2008**, *13*, 116.
[22] M. Haldimann, B. Zimmerli, C. Als, H. Gerber, *Clin. Chem.* **1998**, *44*, 817.
[23] F. Gerondi, M. A. Z. Arruda, *Talanta* **2012**, *97*, 395.
[24] Z. X. Li, L. P. Zhou, F. Tan, *Microchim. Acta* **2006**, *156*, 263.
[25] H. H. Nadiki, M. A. Taher, H. Ashkenani, I. Sheikhshoai, *Analyst* **2012**, *137*, 2431.
[26] Z. Huang, Z. Zhu, Q. Subhani, W. Yan, W. Guo, Y. Zhu, *J. Chromatogr. A* **2012**, *1251*, 154.
[27] E. M. Nolan, S. J. Lippard, *Chem. Rev.* **2008**, *108*, 3443.
[28] D. W. Doraille, E. L. Que, C. J. Chang, *Nat. Chem. Biol.* **2008**, *4*, 168.
[29] L. Tang, Z. Zheng, Y. Bian, *Luminescence* **2016**, *31*, 1456.
[30] T. Wei, H. Li, Q. Wang, T. Lu, Y. Zhu, Q. Lin, Y. Zhang, *Supramol. Chem.* **2016**, *29*, 153.
[31] J. H. Kang, S. Y. Lee, H. M. Ahn, C. Kim, *Sensors Actuators B* **2017**, *242*, 25.
[32] L. Wang, W. T. Li, W. J. Qu, J. X. Su, Q. Lin, T. B. Wei, Y. M. Zhang, *Supramol. Chem.* **2017**, *29*, 489.
[33] A. Paul, S. Anbu, G. Sharma, M. L. Kuznetsov, M. F. C. Guedes da Silva, B. Koch, A. J. L. Pombeiroa, *Dalton Trans.* **2015**, *44*, 16953.
[34] S. A. Lee, J. J. Lee, J. W. Shin, K. S. Min, C. Kim, *Dyes Pigm.* **2015**, *116*, 131.
[35] K. Velmurugan, A. Thamilselvan, R. Antony, V. R. Kannan, L. Tang, R. Nandhakumar, *J. Photochem. Photobiol., a* **2017**, *333*, 130.
[36] H. Goh, T. K. Nam, A. Singh, N. Singh, D. O. Jang, *Tetrahedron Lett.* **2017**, *58*, 1040.
[37] N. S. HariNarayanaMoorthy, V. Pratheepa, M. J. Ramos, V. Vasconcelos, P. A. Fernandes, *Curr. Drug Targets* **2014**, *15*, 681.
[38] S. Banerjee, *ARKIVOC* **2016**, 82.
[39] T. B. Wei, W. T. Li, Q. Li, W. J. Qu, H. Li, G. T. Yan, Q. Lin, H. Yao, Y. M. Zhang, *RSC Adv.* **2016**, *6*, 43832.
[40] G. Y. Gao, W. J. Qu, B. B. Shi, P. Zhang, Q. Lin, H. Yao, W. L. Yang, Y. M. Zhang, T. B. Wei, *Spectrochim, Acta Part a: Mol. Biomol. Spectrosc.* **2014**, *121*, 514.
[41] K. Aggarwal, J. M. Khurana, *J. Lumin.* **2015**, *167*, 146.
[42] J. X. Wang, J. C. Chen, Z. J. Li, *Chin. Sci. Bull.* **1966**, *17*, 419.
[43] A. B. Korzhenevskii, L. Markova, S. V. Efimova, O. I. Koifman, E. V. Krylova, *Russ. J. Gen. Chem.* **2005**, *75*, 980.

[44] A. M. Amer, A. A. El-Bahnasawi, M. R. H. Mahran, *MonatshefteFürChemie* **1999**, *130*, 1217.
[45] International Conference on Harmonization (ICH) of Technical Requirements for Registration of Pharmaceuticals for Human Use Topic Q2 (R1): Validation of Analytical Procedures: Text and Methodology. http://www.ich.org **2005**.
[46] H. Benesi, J. Hilderbrand, *J. Am. Chem. Soc.* **1949**, *71*, 2703.
[47] F. Neese, Orca 3.0.3; max Planck Institute for Bioinorganic Chemistry: Mlheim/Ruhr, Germany. https://orcaforum.cec.mpg.de.
[48] A. Schaefer, H. Horn, R. Ahlrichs, *J. Chem. Phys.* **1992**, *97*, 2571.
[49] F. Weigend, R. Ahlrichs, *Phys. Chem. Chem. Phys.* **2005**, *7*, 3297.
[50] A. Schaefer, C. Huber, R. Ahlrichs, *J. Chem. Phys.* **1994**, *100*, 5829.
[51] D. Andrae, U. Haeussermann, M. Dolg, H. Stoll, H. Preuss, *Theor. Chim. Acta* **1990**, *77*, 123.
[52] F. Weigend, *Phys. Chem. Chem. Phys.* **2006**, *8*, 1057.

## SUPPORTING INFORMATION

Additional supporting information may be found online in the Supporting Information section at the end of this article.

**How to cite this article:** Dongare PR, Gore AH, Kolekar GB, Ajalkar BD. A Phenazine based colorimetric and fluorescent chemosensor for sequential detection of $Ag^{+}$ and $I^{-}$ in aqueous media. *Luminescence*. 2019;1–12. https://doi.org/10.1002/bio.3718